Supplemental Document

Optics EXPRESS

Continuous fabrication of polarization maintaining fibers via an annealing improved infinity additive manufacturing technique for THz communications: supplement

GUOFU XU AND MAKSIM SKOROBOGATIY*

Department of Engineering Physics, École Polytechnique de Montréal, Montreal, Québec, H3T 1J4, Canada
*maksim.skorobogatiy@polymtl.ca

Supplement DOI: https://doi.org/10.6084/m9.figshare.22294057

Parent Article DOI: https://doi.org/10.1364/OE.486400

Continuous Fabrication of Polarization Maintaining Fiber via Annealing Improved Infinity Additive Manufacturing technique for THz Communications: supplemental materials

GUOFU XU AND MAKSIM SKOROBOGATIY*

Department of Engineering Physics, École Polytechnique de Montréal, Montreal, Québec, H3T 1J4, Canada

*maksim.skorobogatiy@polymtl.ca

1. Theoretical Fiber Structure Optimization

The optimization of the fiber structure was conducted using finite element COMSOL Multiphysics software. Infinite lossless air cladding and half computational cell with Perfect Magnetic Conductor (PMC) or Perfect Electric Conductor (PEC) boundary conditions set along the symmetry reflection plane (ZOX) were used to study the lowest order mode featuring electric field directed preferentially parallel (X-polarized) or perpendicular (Y-polarized) to the plane. The effective refractive index and absorption coefficient (by power) of the Polypropylene (PP) polymer were fixed at 1.485 and 2.36 dB/m respectively for 128 GHz, which is the frequency of highest emission intensity of our communication setup. The following fiber geometry optimization was performed for this operating frequency.

It should be also noted that the X-polarized mode generally has a higher excitation efficiency and smaller transmission loss compared with the Y-polarized mode for the proposed fiber design. Therefore, to achieve a longer communication link and better communication quality, our optimization process was mainly focused on the X-polarized mode and the birefringence of the fiber. It should be also noted that the dispersion of the Y-polarized mode can always be at a relatively small value (~1-2 ps/THz/cm) when the dispersion of the X-polarized mode was optimized to be close to zero at 128 GHz. Therefore, our strategy of focusing on optimizing the dispersion of the X-polarized mode can enable both modes of the PMF to simultaneously support high communication bit rates at the carrier frequency of 128 GHz (see Section 3.3 for details).

The hexagonal structure of the fiber is adopted to ease fabrication using the infinity 3D printer without any supporting structure. The size of the fiber square fiber d_c was varied between 0.8-3.2 mm with a minimum step value of 0.1 mm for tuning the spectral position of the zero-dispersion frequency. The bridge width W_b was varied between 0.4-0.8 mm with a step value of 0.1 mm and the bridge inclination θ_b was varied between 2-30 degrees with a minimum step value of 1 degree, to provide sufficient mechanical support between the fiber core and shell while achieving relatively high birefringence. The size D_t of the hexagonal cladding tube was decreased from 9 to 5 mm with a minimum step value of 0.1 mm, to find a design with high flexibility (smaller tube size), while also accommodating the mode field fully inside the fiber outer shell.

The thickness of the hexagonal cladding tube W_t was initially fixed at 0.2 mm as this is the minimum extruder dimension of our infinity 3D printer. Then, by varying $d_c$while fixing the different combination values for W_b, θ_b and D_t, the fiber design featuring near-zero dispersion at 128 GHz for the X-polarized mode can be obtained when d_c=1.6 mm. Since the fiber was designed to be fabricated without the need for a supporting structure, the fiber's outer shell plays an important role in supporting the entire structure during the printing process. As a result, the fiber shell thickness W_t has a great influence on the fiber strength and printing quality, while it is experimentally found that W_t=0.2 mm was not sufficient to provide sufficient stability and strength for the fiber structure during printing. Therefore, to improve the producibility and mechanical strength of the fiber, the W_t was increased from 0.2 mm to 0.4 mm. Meanwhile, however, it was theoretically found that a thicker fiber shell has a strong effect on fiber dispersion when the shell size D_t is smaller than ~6 mm, which can increase the dispersion from near zero to ~2-3 ps/THz/cm at 128 GHz. This negative effect can be mitigated by increasing D_t to 6.8 mm. Therefore, the optimal D_t was chosen to be 6.8 mm, which presents a good compromise between mechanical flexibility and modal confinement/dispersion. With so fixed values of $d_c = 1.6$ mm and $D_t = 6.8$ mm, those dispersion optimized fiber featuring different combination values of W_b and θ_b can achieve a weak sensitivity to the thickened fiber shell W_t. Finally, for the dispersion-optimized fibers with d_c=1.6 mm, $D_t = 6.8$ mm, and W_t =0.4 mm, we then searched for the different combinations of W_b and θ_b to find the fiber with the highest birefringence, which resulted in the choice of W_b=0.5 mm and θ_b=8°.

2. Modal structure of the bent PMF

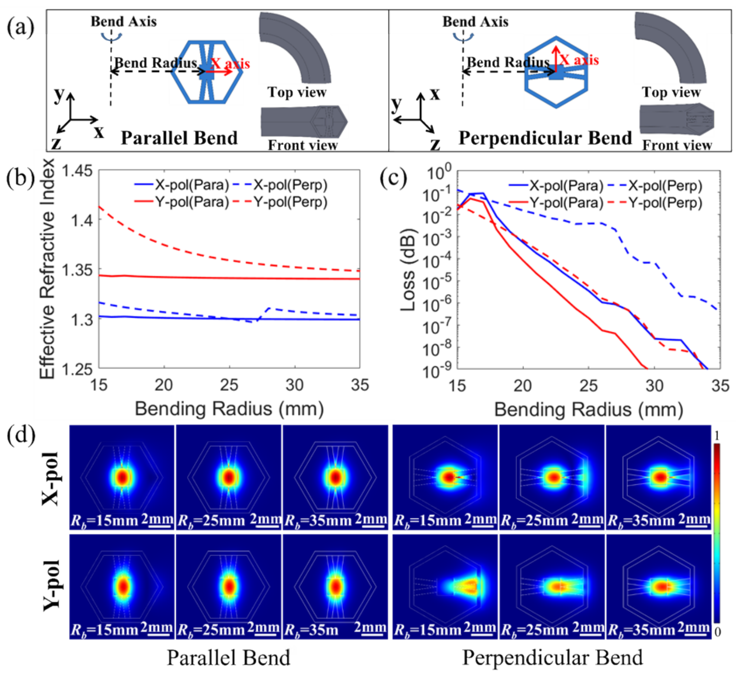

Fig. S1. (a) Schematics of the two types of 90° bends with a 15 mm bending radius for the proposed PMF. (b) Theoretical effective refractive indices and (c) bending losses per 90° bend (by power) of the X-polarized and Y-polarized modes for the two types of bends as a function of the bending radius at 128 GHz. (d) Normalized electric field distributions of the X-polarized and Y-polarized modes for the two types of bends as a function of the bending radius at 128 GHz.

The complex dispersion relations of the X-polarized and Y-polarized modes for the two orthogonal PMF bending directions were studied using COMSOL Multiphysics (axis-symmetric 2D model) by assuming the fiber material as lossless. The schematics of the two orthogonal bending directions for both modes, parallel and perpendicular to the X-axis of PMF, are present in Fig. S1(a), in which the bending radius (R_b) is defined as the distance between the fiber center and the bend axis.

The theoretical effective refractive indices and bending losses of the X-polarized and Y-polarized modes at 128 GHz for the two bend types with the bending radii R_b varying between 15-35 mm are presented in Figs. S1(b) and S1(c), in which the significant increase in the modal effective refractive indices and losses can be observed with the tightened bending radius. This is due to the increased modal presence in the plastic fiber outer shell, bridges, and core regions for tighter bends, which can be seen from the modal field distributions presented in Fig. S1(d). Moreover, it can be found that the parallel bend has less effect on the modal refractive index and losses than the perpendicular bends for both modes [see Figs. S1(b) and S1(c)]. This is attributed to anisotropy in the fiber geometry as the modal fields of both polarization modes can be strongly confined in the core region [see Parallel Bend in Fig. S1(d)] by the high core/air refractive index contrast as the bend radial direction is perpendicular to the core boundary when the PMF was bent along the ZOX plane [left panel in Fig. S1(a)]. In contrast, the modal fields will be easier to leak out through the bridge [see Perpendicular Bend in Fig. S1(d)] as the bend radial direction is parallel to the core-to-bridge region when the PMF was bent along the ZOY plane [right panel in Fig. S1(a)]. Furthermore, compared to the Y-polarized mode, the X-polarized mode is more loosely confined in the core region, thus leading to the highest bending loss in the case of PMF bending along the ZOY plane [blue dashed curve in Fig. S1(c)]. Nevertheless, bending loss smaller than ~0.1 dB per 90° bend can be achieved by both polarization modes in both bend types when the bending radius is larger than ~16 mm, while it is approaching less than ~0.01 dB per 90° bend when bending radius beyond ~20 mm. Therefore, in terms of bending loss, it can be concluded that the proposed PMF can readily tolerate tight bends with a radius as small as ~20 mm, resulting in only a small loss increase of less than ~0.01 dB per 90° bend.

3. The mechanism behind the improvement of fiber quality via annealing

Due to the layer-by-layer deposition nature of the infinity 3D printing technique, surface roughness with dimensions comparable to the thickness of the deposited layer and accidental air trapping are unavoidable, thus leading to additional transmission losses. We have experimentally demonstrated that the fiber transmission loss can be significantly reduced by ~2.7-4.4 dB/m and ~3.8-5.6 dB/m for X and Y polarized modes respectively over 110-150 GHz via annealing the printed fiber at a temperature close to its melting point (see Section 4.2 for fiber quality improvement). To understand the mechanism behind this improvement, two experiments dedicated to studying the internal and surface improvements of the infinity 3D printed fiber were conducted.

Firstly, a study on the surface roughness improvement of the two exposed fiber core walls with annealing time was carried out using the Dektak 150 Surface Profiler (from Veeco, Inc). The measurement was performed along the direction of material layer deposition for each wall [see red arrows in Figs. S2(a) and S2(b)]. In each measurement, five different locations along the exposed core walls of the whole fiber section (25 cm long) were inspected to obtain the representative surface roughness. Then the exposed fiber core was annealed in a vacuum furnace at ~140℃ for 24 hours and the measurement was repeated after the fiber core is sufficiently cooled down. The surface roughness measurement and annealing were alternately repeated 5 times. It should be noted that the annealing temperature was experimentally found to allow the fiber to soften enough while avoiding any structural deformation [see Fig. S2(c)]. Thus, the representative surface roughness distributions and microscopic images of the PMF core walls annealed for different days (0-5 days) are presented in Figs. S2(a) and S2(b), in which the root mean square average of the profile heights over the evaluation length also known as the roughness Rq is displayed.

It was experimentally found that the surface roughness of the infinity-printed PMF core walls before annealing is ~35 μm, which is ~10-15 μm higher than the wall roughness of the fiber printed with standard 3D printers (see our previous work presented in [1]). After 2 days of annealing, the surface roughness of the two core walls was reduced by ~5 μm, with minor improvements in the following 3 days of annealing. The improved surface roughness of the infinity 3D printed fiber core walls after 5 days of annealing is in the range of ~27-30 μm, which is still slightly higher than the ~20-25 μm roughness of walls printed with standard 3D printers.

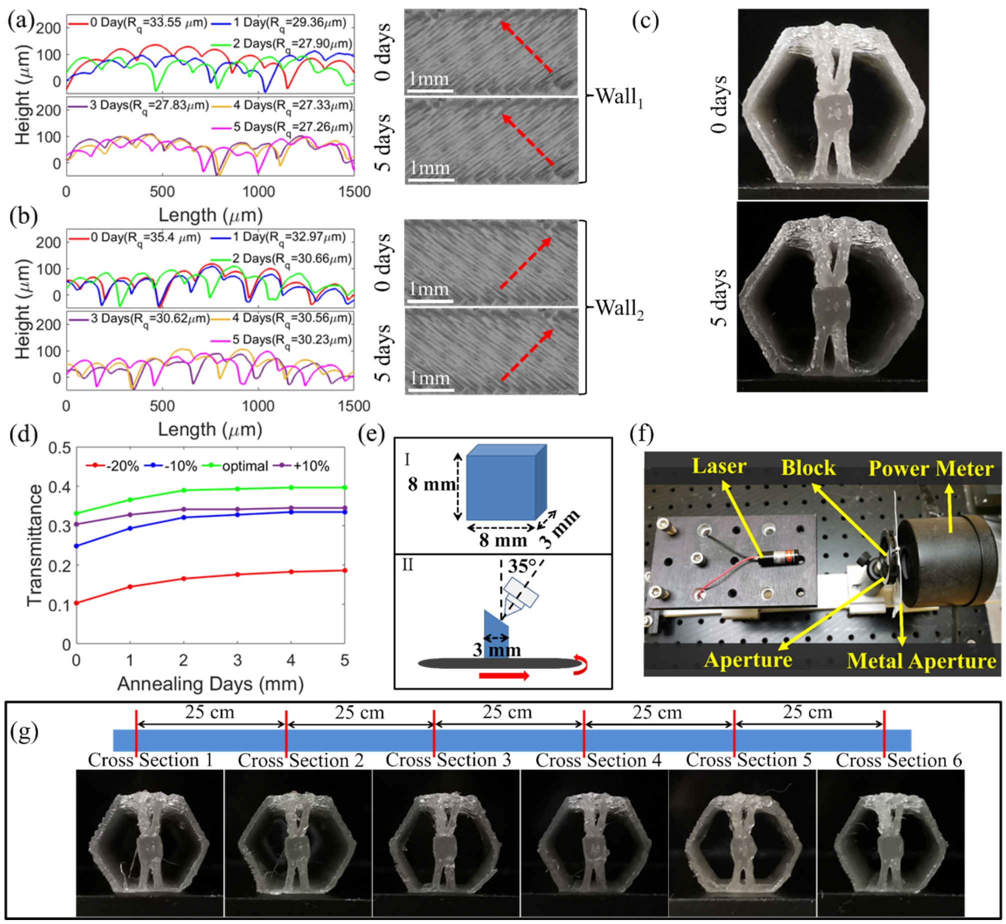

Fig. S2.(a)(b) Typical surface roughness distributions and microscopic images of the two exposed PMF core walls annealed for 0-5 days. The red arrows indicate the corresponding profiling directions. (c) The microscopy images of the PMF crosssections before and after annealing. (d) The transmittance of the square blocks printed with different infill flow rates as a function of the annealing time. (e) Schematics of the blocks and their fabrication process. (f) Experimental setup for measuring the transmittance of the 3D printed blocks. (g) The microscopy images of the PMF crosssections and their corresponding locations along the fiber length.

Next, the interior improvement of the printed fibers with annealing time was studied by measuring the optical transmission of a 650 nm laser through the infinity 3D printed blocks [Fig. S2(e)]. As shown in Fig. S2(f), an aperture (IDA25 from Thorlabs, Inc) and a metal plate with a square hole were used to fix the printed blocks and prevent the stray light, a laser (FU650AD5-BC10/BD10) was used to launch the beam through the block, while the intensity of the transmitted light was measured using a power meter (P/N 1Z01500 from Nova Display Systems, Inc). The transmittances of the four blocks printed with different infill flow rates were obtained by normalizing the intensity of the light transmitted through the blocks to that of the empty system. Similar to the surface roughness measurement, the transmittance of the four blocks was remeasured after every 24 hours of annealing. Thus, the normalized transmittances of the blocks as a function of annealing time are presented in Fig. S2(d), from which we can see that the transmittance of all the blocks can be greatly improved after 2 days of annealing, which is similar to the surface roughness improvement and also accordance with the loss measurements of three fiber sections (see Section 4.2). In addition, we can also see that the block printed with the optimal infill flow rate still has the highest transmittance after annealing, which indicates that the optimization of printing parameters is still the primary method for improving print quality and annealing can be used as a compensatory method for further improvement. For the blocks printed with the suboptimal infill flow rates [indicated as optimal-20% in Fig. S2(d)], it seems that annealing can continuously improve the transmittance beyond 5 days of annealing. This is because for suboptimal infill flow rates more air is trapped inside the bulk material, resulting in a longer time required to adequately mitigate the defects.

We can, thus, conclude that, by annealing the fiber at a temperature close to its melting point, both the surface roughness and transmittance of the bulk material region can be improved, which therefore leads to a significant reduction in the fiber transmission loss. Although the transmission loss of the annealed infinity 3D printed PMF fibers is still at least ~2 dB/m higher than those printed using a standard 3D printing process, this is attributed to the slightly rougher surface, as well as the relatively stronger variations in the fiber cross-section geometry along the fiber length (compared to standard printed fibers) as surmised from the cross-sectional images of the fiber sections obtained from the cut-back measurement [see Fig. S2(g)]. We believe that such fabrication imperfections can be mitigated by using deeper process optimization procedures with finer control over more factors such as ambient temperature stability and stress at the interface between the fiber and the conveyor belt of an infinity printer that are not adequately considered in current commercial printers. Therefore, we believe that high-quality THz fibers with a much smaller surface roughness of ~15 μm and highly constant longitudinal quality are achievable by using a fully developed 3D printer combined with an annealing technique, which makes it a competitive alternative to fiber drawing and extrusion as fiber profiles unlimited in complexity can be fabricated without any process development.

4. Continuous wave THz spectroscopy system to measure the fiber loss and crosstalk

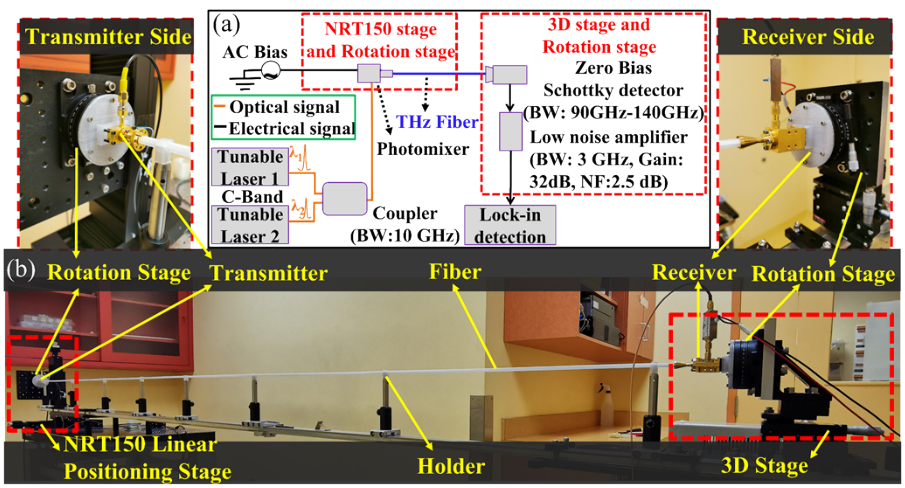

Fig. S3. (a) Schematic of the CW THz spectroscopy system. (b) Experimental setup to measure the transmission loss and crosstalk of the PMF (3 m-long). Inset: the enlarged view of the transmitter (WR-6 rectangular flange mounted) and receiver (horn antenna mounted) side.

The transmission loss and crosstalk of the X-polarized and Y-polarized modes of the PMF were characterized by using the Continuous Wave (CW) THz spectroscopy system. The system schematic and experiment setup are shown in Fig. S3. The CW THz spectroscopy system can be briefly described as follows: On the transmitter side, two tunable lasers (TeraBeam) operating at judiciously mismatched wavelengths are used to optically drive the THz photomixer for the difference frequency generation of THz waves. The generated THz wave from the photomixer (Model: IOD-PMD-14001from NTT Electronics, Inc) is guided inside a

WR-6 rectangular waveguide flange, which is butt-coupled to the fiber under study. On the receiver side, a 10.8 mm diameter horn antenna is attached to the zero bias Schottky detector (Model: WR8.0 ZBD-F from Virginia diodes, Inc) for THz signal detection. A high gain low noise amplifier (Model: SLNA-030-32-30-SMA from Fairview Microwave, Inc) is then used to amplify the received signal for further signal processing.

To selectively characterize the X-polarized and Y-polarized modes, both the transmitter and receiver were mounted on the manual High-Precision Rotation Stages (PR01 from Thorlabs, Inc) for precisely aligning the electric field directions between the excitation beam and the two orthogonally polarized fundamental modes of the PMF. Moreover, the rotation stage with the receiver was mounted on a 3D linear positioning stage (RBL13M from Thorlabs, Inc) for manual optimizing the relative position between the receiver and fiber output, thus maximizing the received THz signal. Meanwhile, another rotation stage with a transmitter was mounted on a 3D computer-controlled linear positioning stage featuring on-axis accuracy of 2 µm (NRT150 from Thorlabs, Inc) to optimize and maintain the excitation arrangements (position and inclination) for X-polarized and Y-polarized modes respectively. Before conducting the experiments, the inclinations of both transmitter and receiver were simultaneously optimized at the same angle with a minimal step value of 2 degrees. For each inclination, the position of the transmitter was optimized using the computer-controlled stage and then the position of the receiver was optimized manually to maximize the received signal. Finally, the optimal excitation inclinations for X-polarized and Y-polarized modes were found to be in the horizontal (0°) and vertical (90°) directions, and the best excitation positions of the transmitter were also identified and marked as $P_x\,(x_1,y_1,z_1)$ and $P_y\,(x_2,y_2,z_2)$.

Then, the experiments for measuring the transmission loss and crosstalk were carried out starting from the fiber length of 3 m. For each measurement, the inclination and position of the transmitter were firstly set as 0° and P_x to optimally excite the X-polarized mode. While the inclination of the receiver was set to either 0° or 90° to record the signals carried by the two orthogonally polarized modes. Furthermore, the position of the receiver was optimized manually for each inclination (0° and 90°) to maximize the received signals. Next, the inclination and position of the transmitter were adjusted to 90° and P_y to optimally excite the Y-polarized mode, and the optimization procedure of the receiver was repeated. Next, the fiber was cut and the above procedures were repeated until the fiber was cut down to 1.6 m, with the output signal strength sufficient to conduct the THz communication studies. It should be noted that the fiber input end was always fixed and unaltered throughout the measurement, while the inclination and position of the transmitter were switched between the optimal excitation arrangements of the X-polarized and Y-polarized modes by using the high-precision rotation stage and a linear positioning stage. Therefore, the optimal excitation arrangements (position and inclination) for both modes were maintained and fixed throughout the experiment.

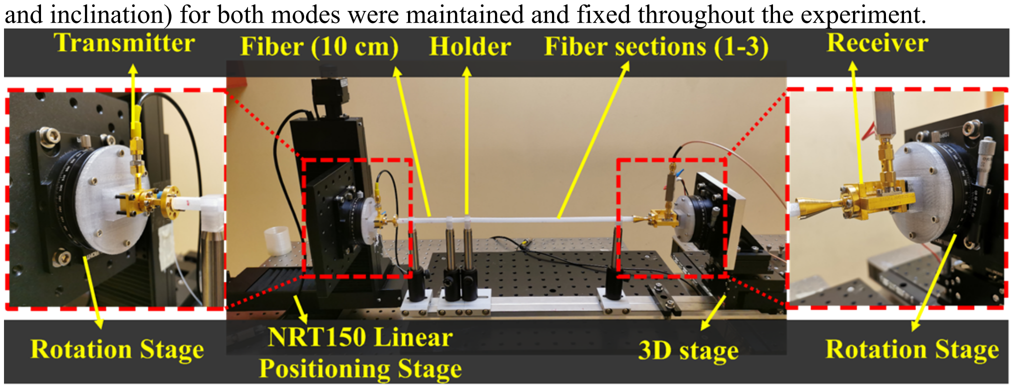

Fig. S4. Experimental setup to measure the losses of three 25 cm-long PMF fiber sections before and after annealing. Inset: the enlarged view of the transmitter (WR-6 rectangular flange mounted) and receiver (horn antenna mounted) side.

The experiment setup shown in Fig. S4 is similar to that of Fig. S3, the difference is that the losses of the three 25 cm-long fiber sections (see Section 4.2) annealed for 0-5 days were measured by comparing the reference signal at the fiber input end with the signal at the fiber output end. The reference signals (X and Y polarizations) were recorded at the output end of a 10 cm-long fiber section which was always fixed throughout the experiment, the position and inclination of the transmitter were maintained at the optimal excitation conditions for each polarization. The three 25 cm-long fiber sections were annealed in the vacuum furnace for 1-5 days at a temperature close to the melting point (~ 150 ℃) of the material (PP). Then, the annealed fiber sections were taken out every 24 hours and mechanically spliced with the 10 cm-long fiber using the hexagonal holder/connecter for measuring the output signal. For each measurement, the position and inclination of the receiver were optimized to maximize the received signal.

5. Photonics-based THz communication system and bit error measurement

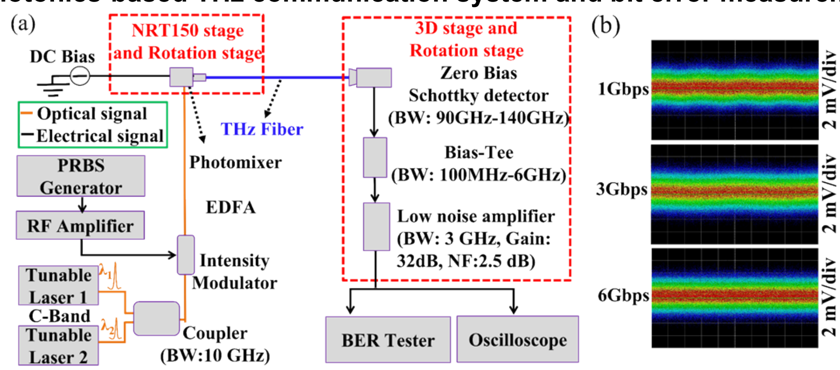

Fig. S5. (a) Schematic of the photonics-based THz communication system. (b) Eye patterns of the system noise floor (no signal) at different bit rates.

The bit error rate (BER) measurement was carried out using the photonics-based THz communication system. The schematic of the THz communication system is shown in Fig. S5(a) and briefly described as follows: For the transmitter side, an external electro-optic modulator (Model: LN81S-FC and MX10A from Thorlabs, Inc) was employed to modulate the infrared optical signals, a non-return-to-zero (NRZ) pseudo-random bit sequence (PRBS) digital signal with a pattern length of 2^{31}-1 was used as the baseband signal. While for the receiver side, a Bias-Tee was added before the low noise amplifier, a high-speed oscilloscope and BER tester (Model: MP2100B from Anritsu Corporation) was utilized to analyze the received and demodulated baseband signals. The 3D printed fiber, the transmitter, and the receiver antennas were in the same arrangements as the transmission loss measurement [see Fig. S3(b)]. At each bit rate, the decision threshold was optimized to obtain the minimum BER[2]. The target BER of an error-free transmission was set to 10^{-12}, and the measurement duration is inversely proportional to the bit rate [1/(target BER ∗ bit rate)].

In Fig. S5(b) we present the eye patterns for the noise floor of our communication system. Here, the noise floor is the amplitude of the eye diagram without any input signal, which is defined as the distance between the mean one and mean zero levels. Therefore, the noise floor of our communication system was measured to be 2.08 mV, 2.22 mV, and 2.14 mV for the bit rates of 1 Gpbs,3 Gpbs, and 6 Gpbs, respectively.

6. Experiment setup for modal field imaging

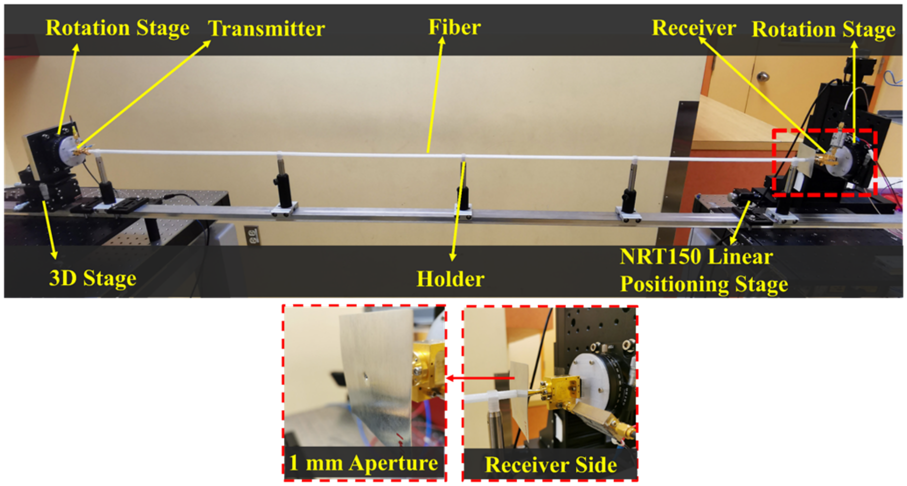

Fig. S6. Experimental setup for the near-field THz modal imaging of the PMF (1.6 m). Inset: the enlarged view of the receiver side with subwavelength (~1 mm) aperture mounted on the horn antenna.

The mode field imaging for the X-polarized and Y-polarized modes of the PMF was carried out by using the CW THz spectroscopy system as shown in Fig. S3(a). Before conducting the mode field imaging, the 3D printed fibers, the transmitter, and the receiver antennas were in a similar arrangement to the transmission loss measurement shown in Fig. S3(b). The difference is that the transmitter was mounted on a manual 3D linear positioning stage for manual optimization of the excitation positions for X-polarized and Y-polarized modes respectively, while the receiver was mounted on a 3D computer-controlled linear positioning stage (NRT150 from Thorlabs, Inc) (see Fig. S6) and a sub-wavelength aperture of ~1 mm diameter (see the Inset of Fig. S6) was attached to the 10.8 mm diameter horn antenna of the receiver to work as a near-field probe. Thus, by raster scanning the fiber output facet with a spatial resolution of 0.3 mm, the modal field profile of 12 mm $\times$ 12 mm area of the fiber cross-section was acquired as 41×41 images. It should be noted that for each modal polarization, the excitation arrangements of the transmitter (inclination and position) were first optimized and then maintained throughout the near-field imaging.

References

1. G. Xu, K. Nallappan, Y. Cao, and M. Skorobogatiy, "Infinity additive manufacturing of continuous microstructured fiber links for THz communications," Scientific reports **12**, 1-13 (2022).
2. K. Nallappan, Y. Cao, G. Xu, H. Guerboukha, C. Nerguizian, and M. Skorobogatiy, "Dispersion Limited versus Power Limited Terahertz Transmission Links Using Solid Core Subwavelength Dielectric Fibers," Photonics Research **8**, 1757-1775 (2020).